MAS Journal of Applied Sciences Uygulamalı Bilimler Dergisi ISSN: 2757-5675 masjaps.com

OPEN ACCESS

DOI: http://dx.doi.org/10.5281/zenodo.14542860

Araştırma Makalesi / Research Article

Digital Mapping of Soil pH and Electrical Conductivity: A Comparative Analysis of Kriging and Machine Learning Approaches

Mustafa ÖZTÜRK [1], Miraç KILIÇ [2], Hikmet GÜNAL [1*]

[1] Harran University, Faculty of Agriculture, Department of Soil Science and Plant Nutrition, Sanliurfa

[2] Malatya Turgut Özal University, Faculty of Agriculture, Department of Soil Science and Plant Nutrition, Malatya

*Corresponding author: hikmetgunal@harran.edu.tr

Received: 20.08.2024 **Accepted**: 05.10.2024

Abstract

Soil pH and electrical conductivity (EC) are critical soil properties influencing agricultural productivity and environmental sustainability. This study evaluates the performance of stacked machine learning models in predicting and mapping soil pH and EC values. Base models such as Ordinary Kriging (OK), Universal Kriging (UK), and Disjunctive Kriging (DK) were employed, and their outputs were integrated into a Multilayer Perceptron (MLP) neural network meta-model. The results reveal the superior performance of the MLP meta-model across all metrics. For instance, in predicting pH, the MLP model achieved an RMSE of 0.028, an MAE of 0.020, and an R^2 of 0.858 on the training dataset. For EC predictions, the MLP model outperformed others on the test dataset, with an RMSE of 0.039, an MAE of 0.028, and an R^2 of 0.900. In contrast, the UK and DK methods exhibited lower accuracy, particularly on test datasets. This study shows the advantage of modern machine learning algorithms in modeling nonlinear spatial relationships and their significant potential in digital soil mapping. The findings demonstrate the applicability of these approaches in enhancing agricultural productivity and supporting sustainable soil management practices.

Keywords: Soil pH, electrical conductivity, machine learning, kriging, digital soil mapping

1. Introduction

Soil pH is a key factor that indicates whether soil is acidic or alkaline and plays a crucial role in shaping various soil properties and processes. Plants have specific pH preferences, and maintaining the appropriate pH range is essential for ensuring nutrient availability to support healthy plant growth (Neina et al., 2019). Soil acidity poses a global challenge, arising from both natural processes and human activities. Naturally, it can result from the leaching of base cations such as calcium, magnesium, and potassium in areas with high rainfall, leaving behind hydrogen and aluminum ions. Other natural contributors include the weathering of minerals, aluminum hydrolysis, plant uptake of cations over anions, and the oxidation of organic matter and sulfur minerals. Human activities also contribute significantly to soil acidification, particularly through the burning of fossil fuels that release sulfur and nitrogen gases, leading to acid rain. Furthermore, the excessive use of ammonium-based fertilizers intensifies the problem (Hue, 2022).

Soil salinity is a significant global concern, affecting more than 900 million hectares of land (Hopmans et al., 2021). This issue is especially harmful in semi-arid and arid regions, where it degrades soil and water quality, hampers seed germination, reduces agricultural productivity, and accelerates land degradation (Singh, 2022). In these areas, conditions such as high rates of evapotranspiration, limited precipitation, and specific soil characteristics promote the accumulation of salts in the soil. The concentration of salts, particularly in the upper soil layers, modifies soil properties and impairs its overall functionality (Butcher et al., 2016).

Soil pH is an important property that directly affects plant growth and development, making its assessment and management critical for agricultural productivity and environmental sustainability (Lu et al., 2023). By monitoring soil pH, farmers can make strategic decisions regarding fertilization and soil management, leading to healthier crops and higher yields (Singh, 2022). Extremely acidic or alkaline soils can hinder nutrient availability, reducing plant productivity, while soil pH also influences microbial activity, a key factor in maintaining soil health (Suarez, 2006).

Under natural conditions, soil pH changes occur gradually, with spatial variability driven by factors such as topography, climate, parent material, vegetation, and human activities (Cannone et al., 2021; Zhao et al., 2024). In contrast, agricultural practices can result in rapid and substantial shifts in soil pH. Understanding these temporal and spatial variations is essential for sustainable agricultural practices. Tools such as Geographic Information Systems and digital soil mapping provide effective means for analyzing and mapping the spatial variability of soil pH (Filippi et al., 2018).

Estimating and mapping soil pH and EC over large areas is essential for efficient resource management and enhancing crop productivity. However, performing these tasks using traditional methods is both time-consuming and costly. Geostatistical methods, particularly kriging interpolation techniques, have long been employed for spatial modeling of soil properties as they enable the prediction of soil parameters across extensive landscapes (Filippi et al., 2018; Lu et al., 2023; Zhao et al., 2024).

In recent years, modern interpolation techniques such as High Accuracy Surface Modeling (HASM) have demonstrated significant advantages in spatial predictions of variables like soil pH. Shi et al. (2009) reported that HASM achieved higher accuracy, with lower MAE (0.16) and RMSE (0.22) values, compared to traditional methods such as kriging, IDW, and splines. Nonetheless, these methods may encounter limitations in capturing complex spatial patterns and minimizing prediction errors.

Recently, machine learning algorithms have emerged as powerful tools for improving prediction accuracy in environmental studies (Günal et al., 2021: Abakay and Günal, 2023; Durmaz et al., 2024). For example, the Random Forest algorithm has been reported to deliver superior performance in predicting soil pH and EC (Lu et al., 2023; Zhao et al., 2024). The careful selection of machine learning algorithms significantly impacts model performance. In a study by Khaledian and Miller (2020), various algorithms were compared in terms of hyperparameter requirements, dataset size, and model interpretability. The Cubist and Random Forest algorithms showed strong performance, particularly with smaller datasets.

Ensemble methods, especially stacked machine learning models, provide a significant advantage by combining multiple base models to harness their individual strengths. The integration of geostatistical techniques with artificial neural network-based meta-models improves the reliability of spatial predictions by effectively addressing both systematic and random errors.

This study investigates the effectiveness of stacked machine learning models in predicting and mapping soil pH and EC. Khaledian and Miller (2020) evaluated machine learning algorithms based on five critical criteria: hyperparameter count, sample size, variable selection, training time, and model interpretability. Their findings highlighted the superior accuracy of Cubist and Random Forest algorithms, even when applied to small datasets. These results served as a foundation for designing the stacked models used in this research. The proposed methodology utilizes Ordinary Kriging (OK), Universal Kriging (UK), and Disjunctive Kriging (DK) as base models, which are then integrated with a Multilayer Perceptron (MLP) neural network serving as the meta-model. This approach introduces an innovative framework for spatial modeling of soil properties, aiming to advance precision agriculture practices.

2. Materials and Methods

2.1. Study area

The study area spans a vast region within Şanlıurfa province, which is known for its prominent pistachio cultivation. Located in southeastern Turkey, Şanlıurfa has a rich geological background, with much of the area composed of limestone, basalt, and alluvial rocks from the Cenozoic era. Limestone formations are especially significant in the province's geology, found primarily in the Fatik Plateau to the north and west and the Tektek Mountains to the east. The Fatik Plateau contains extensive Eocene limestone deposits, often white or yellow in color and highly calcified, while the Tektek Mountains feature younger limestone deposits from the Oligocene-Miocene epochs, generally yellow or brown, with less karstification (Özcan, 1974).

On the geological map of Şanlıurfa, green areas indicate Cretaceous-Paleocene clastic and carbonate rocks, orange areas represent Eocene limestones, and yellow areas correspond to Miocene limestones. These limestones are part of the Midyat Group, which includes formations from the Eocene, Oligocene, and Early Miocene periods. Under the region's arid climate, these limestone formations support xerophytic vegetation, such as maquis and steppe communities.

Şanlıurfa, located in southeastern Turkey, is where the Mediterranean and continental climates meet, resulting in a semi-arid Mediterranean climate. Precipitation is concentrated in the winter months, when temperatures are more moderate. The long-term average annual rainfall is 459.3 mm, which is below the Mediterranean regional average. Most rainfall occurs between November and March, while there is a significant reduction in rainfall during July and August. Summers are hot and dry, with an average annual temperature of 18.5°C. The coldest month is January, with an average temperature of

5.6 °C, while July is the hottest month, with an average temperature of 32 °C. Winters are generally mild, with January being the coldest month, though temperatures rarely drop below freezing. Snowfall is typically observed in December, January, and February, but the snow cover is usually brief. The climate of Şanlıurfa significantly influences its natural vegetation and agricultural practices. Due to the hot, dry summers, the region's vegetation mainly consists of drought-resistant maquis and steppe plants. Agriculture is predominantly focused on irrigated farming during the winter months (MGM, 2024).

2.2. Soil sampling and laboratory analysis

Soil samples were collected from disturbed soils at a depth of 0-20 cm from 104 points, representing three primary land uses: dry farming fields, pasture areas, and pistachio orchards. These points were selected from homogeneous units with areas ≥1 km² (Figure 1). Among the samples, 13 were from fields that had been used for barley, wheat, or other crops like lentils and alfalfa but were not planted at the time of sampling. Additionally, 65 samples were taken from pistachio orchards of various ages, 14 from pasture areas, 8 from cotton fields, and 4 from olive orchards. The coordinates of each sampling point were recorded in the field using a handheld GPS device.

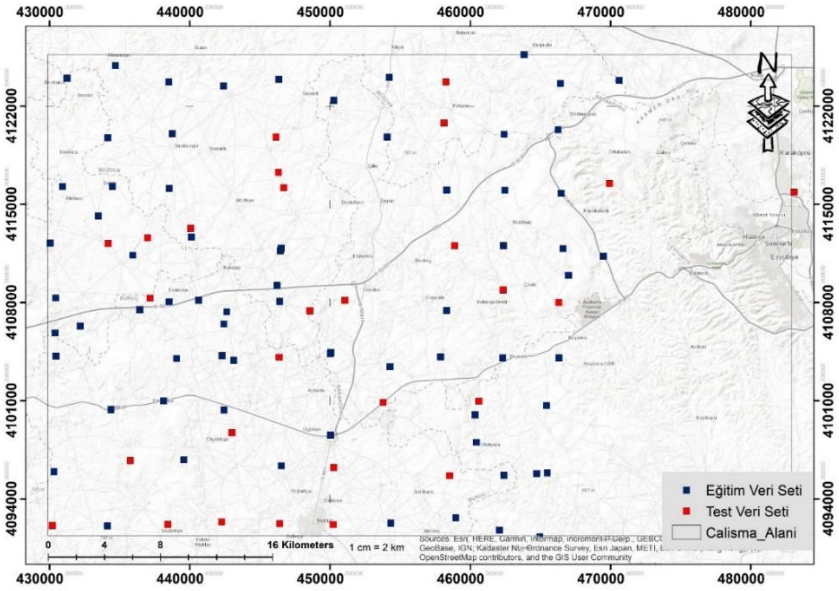

Figure 1. The locations of the soil samples within the study area and their distribution in the test and training datasets of the models

After air-drying, the soil samples were sieved through a 2 mm mesh and prepared for further analysis. Electrical conductivity (EC) and pH were measured in a 1:2.5 soil-water suspension using an EC-pH meter, following the method outlined by the US Salinity Lab Staff (1954).

2.3. Modelling approach

The Stacked Machine Learning Model, also known as stacking or stacked generalization, is an ensemble learning technique that integrates multiple predictive models. The fundamental concept behind stacking is to capitalize on the strengths of various base models (Level 0: Ordinary Kriging, Universal Kriging, and Disjunctive Kriging) and use a meta-model (Level 1: Multilayer Perceptron Neural Network, MLP) to optimally combine their predictions. This two-level approach

enables the meta-learner to correct biases in the base models and reduce both systematic and random errors, thereby enhancing prediction accuracy (Ma et al., 2018; Wang, 2018).

2.3.1. Base models (Level 0)

Ordinary Kriging (OK) is a geostatistical interpolation method used with spatial data and is defined as the Best Linear Unbiased Estimator (BLUE). This method provides a prediction that is "optimal" (minimizing error variance), "linear" (using a weighted linear combination of existing data), and "unbiased" (with an error mean equal to zero). The fundamental principle of Ordinary Kriging is to predict the value of a regionalized variable, $Z(s0)$, at a location to be estimated, based on the surrounding available data. (Equation 1) (Mesić Kiš, 2016; Webster and Oliver, 2007):

$$Z(s_0) = \sum_{\{i=1\}}^{n} \lambda_i Z(s_i) \qquad (1)$$

λi: Weight coefficients,
$Z(s_i)$: Observations at the existing data points,
n: The number of data points used.
These weights are determined to satisfy the conditions of unbiasedness (Equation 2) and minimum variance (Equation 3), as outlined below (Journel and Huijbregts, 1978):

$$\sum_{\{i=1\}}^{n} \lambda_i = 1 \qquad (2)$$

$$min\ VAR\left[Z(s_0) - \sum_{\{i=1\}}^{n} \lambda_i Z(s_i) \right] \qquad (3)$$

To determine the weights, the equation in matrix form from Equation 3 is used (Malvić and Balić, 2009):

$$\begin{bmatrix} \gamma(s_1,s_1) & \gamma(s_1,s_2) & \cdots & \gamma(s_1,s_n) & 1 \\ \gamma(s_2,s_1) & \gamma(s_2,s_2) & \cdots & \gamma(s_2,s_n) & 1 \\ \vdots & \vdots & \ddots & \vdots & \vdots \\ \gamma(s_n,s_1) & \gamma(s_n,s_2) & \cdots & \gamma(s_n,s_n) & 1 \\ 1 & 1 & \cdots & 1 & 0 \end{bmatrix} \cdot \begin{bmatrix} \lambda_1 \\ \lambda_2 \\ \vdots \\ \lambda_n \mu \end{bmatrix} = \begin{bmatrix} \gamma(s_1,s_0) \\ \gamma(s_2,s_0) \\ \vdots \\ \gamma(s_n,s_0) 1 \end{bmatrix} \quad (3)$$

Where:

$\gamma(s_i,s_j)$: represents the semivariogram value between the points si and sj,
μ: Lagrange multiplier.

Universal Kriging (UK) is a geostatistical method employed for spatial data prediction when a significant trend is present in the data. It is particularly useful when the mean of the variable is not constant, meaning the stationarity assumption is violated. Universal Kriging decomposes the predicted variable into two components: a deterministic function (μ(x)), which represents the significant trend, and a random component (Y(x)), as expressed in Equation 4 (Wackernagel, 2003):

$$Z(x) = \mu(x) + Y(x) \quad (4)$$

Where:

$Z(x)$: The regionalized variable at location x,
$\mu(x)$: the deterministic trend that varies with spatial location,
$Y(x)$: the random component, which is considered a stationary process.

The trend component (μ(x)) is modeled as a polynomial function, which is represented in Equation 5. This polynomial function captures the underlying trend in the data, accounting for spatial variations that cannot be explained by the random component alone (Kumar, 2007):

$$\mu(x) = \sum_{l=1}^{k} \alpha_l f_l(x) \quad (5)$$

Where:

α_l: The coefficients to be predicted from the data,
$f_l(x)$: the basic function that defines the spatial coordinates,
k: the number of functions used to model the trend.

Disjunctive Kriging (DK) relies on the principle of transforming the data into standard normal variables using Hermite polynomials and then applying the kriging method to predict these polynomials. The predicted values are subsequently inverse-transformed to obtain results in the original units of the variable (Olıver et al., 1996). DK expresses the prediction of a variable using the equation provided in Equation 6:

$$Z_{DK}(x) = \sum_{k=0}^{\infty} \phi_k H_k\big(Y(x)\big) \quad (6)$$

$$\phi_k = \int_{-\infty}^{\infty} Z(x) H_k\big(Y(x)\big) g\big(Y(x)\big) dY \quad (7)$$

Where:
Z_{DK}(x): Estimated value,
ϕ_k: Hermite coefficients,
Hk(Y(x)):The k-th Hermite polynomial of Y(x)

2.3.2. Level 1

The Multilayer Perceptron Artificial Neural Network (MLP-ANN) is a type of artificial neural network that consists of an input layer, one or more hidden layers, and an output layer. It functions through supervised learning, where it learns the nonlinear relationships between the input variables and the target outputs. Each layer is made up of nodes (neurons), which are processed with weights and biases (Pinkus, 1999). A multilayer MLP is represented by Equation 8 (Haykin, 1999):

$$\widehat{y^{(l)}} = f\left(W^{(l)}\widehat{y^{(l-1)}} + b^{(l)}\right) \quad (8)$$

Where; $W^{(l)} ve\ b^{(l)}, l -$ represents the weight matrix and bias vector of the n n-th layer.

GridSearchCV is a methodical approach used for hyperparameter optimization of machine learning models, and it was applied in this study to enhance the performance of the MLP-ANN model. This method tests different combinations of predefined hyperparameters via a grid search and evaluates the accuracy of each combination using k-fold cross-validation (Kong et al., 2024). In this study, GridSearchCV was implemented with 5-fold cross-validation to optimize hyperparameters specific to the MLP-ANN model, such as 'activation', 'alpha', 'hidden_layer_sizes', and 'solver', with error metrics used to assess the model's performance.

For this study, the outputs from the Level 0 base models were used as input data (common variables) for the Level 1 meta-model. The dataset was split into 70% for training and 30% for testing at both levels (Figure 1). The Level 0 Kriging models and the Level 1 MLP models were both trained using the training dataset. While the Level 0 models were generated using ArcGIS 10.8 Geostatistical Wizard, the Level 1 model was developed in Python 3.8 using the Scikit Learn library.

2.4. Accuracy assessment

Root Mean Squared Error (RMSE) is designed to compare the final predicted output with the target output and is a performance metric calculated from the differences between the network's output and the target. RMSE is inversely proportional to prediction accuracy (a larger RMSE value indicates lower prediction accuracy). The RMSE value is calculated using the following equation *;

$$RMSE = \sqrt{\frac{1}{n}\sum_{t=1}^{n}(E_i - M_i)^2} \quad (9)$$

Where RMSE (Root Mean Square Error) is the square root of the average squared error, E_i, M_i and n represent the predicted values, measured values, and the number of samples, respectively. To evaluate the prediction performance of each model at different levels, three validation indices defined by Isaaks and Srivastava (1988)—Mean Absolute Error (MAE) and Root Mean Square Error (RMSE)—are calculated using the following equations:

$$ME = \frac{1}{n}\sum_{i=1}^{n}[\hat{Z}(x_i) - Z(x_i)] \quad (10)$$

$$MAE = \frac{1}{n}\sum_{i=1}^{n}\left|\hat{Z}(x_i) - Z(x_i)\right| \quad (11)$$

$$R^2 = 1 - \frac{\sum_{i=1}^{n}(z_i - \hat{z_i})^2}{\sum_{i=1}^{n}(z_i - z)^2} \quad (12)$$

In the equation; $\hat{Z}(x_i)$ represents the predicted soil properties (such as pH or EC), $Z(x_i)$ refers to the measured soil properties, and n is the number of samples used for validation.

3. Results and Discussion

3.1. Statistical analysis

When comparing the statistical properties of soil pH and electrical conductivity (EC) values between the training and test datasets, several similarities and differences were observed (Table 1). For pH values, there were no significant statistical differences between the two datasets, both showing similar distributions. The mean pH value for both the training and test datasets was 7.78. However, the standard deviation for the training dataset was 0.09, slightly higher than the test dataset's standard deviation of 0.08, suggesting slightly more variability in the training data's pH values.

For EC values, the mean in the training dataset was 0.44, while the test dataset's mean was 0.45. However, the coefficient of variation for EC was higher in the test dataset (31.45%) than in the training dataset (24.27%), indicating that the EC values in the test data exhibited greater variability. These findings suggest that the training and test datasets may exhibit different characteristics during model validation, with the test dataset, particularly for EC predictions, requiring more careful analysis.

Table 1. Statistical properties of soil pH and EC values for training and test data

	Training		Test	
	pH	**EC**	**pH**	**EC**
Number of Samples	70	70	30	30
Mean	7.78	0.44	7.78	0.45
Standard Deviation	0.09	0.11	0.08	0.14
Minimum	7.45	0.275	7.58	0.282
Maximum	7.95	0.784	7.92	0.947
Coefficient of Variation (%)	1.16	24.27	0.99	31.45

3.2. Model parameters

In this study, the spatial distribution of soil pH and EC was modeled using digital soil mapping techniques and machine learning algorithms. The first stage of spatial modeling for soil pH, referred to as Level 0 (base models), was performed using three different kriging interpolation methods: Ordinary Kriging (OK), Universal Kriging (UK), and Disjunctive Kriging (DK), which aim to capture distance-dependent variations in soil properties. The semivariogram parameters and spatial dependence rates for soil pH and EC values, based on the OK, UK, and DK methods, are summarized in Table 2. The spatial dependence rate is defined as the ratio of the nugget to the sill and is interpreted according to the classification proposed by Camberdella (1994). According to this classification, a spatial dependence rate of <25% indicates strong spatial dependence, between 25-75% indicates moderate spatial dependence, and >75% indicates weak spatial dependence.

For the analysis of pH values, the OK method showed a nugget value of 0.0000258017, a partial sill value of 0.00010771, and a total sill value of 0.00013351, resulting in a spatial dependence rate of 80.7%, which indicates weak spatial dependence. The range value of 5530 m suggests a moderate effect distance. The UK method produced a nugget value of 0.0011356647, a partial sill value of 0.00682873, and a total sill value of 0.0079644. With a spatial dependence rate of 85.7%, it also indicated weak spatial dependence, suggesting that pH values are distributed homogeneously over a wide spatial area. The range value of 5530 m was consistent with that of the OK method. In the DK method, the nugget value was 0.2352803000, the partial sill value was

0.767537, and the total sill value was 1.0028173, indicating higher variation in pH values. The spatial dependence rate for DK was 76.5%, also indicating weak spatial dependence. The range value of 5050 m suggested a shorter effect distance compared to the OK and UK methods. These results indicate the variations in the spatial distribution of soil pH across different kriging methods, offering unique insights into the spatial structure of the data.

In the analysis of EC values, for the OK method, the nugget value was calculated as 0.0061058190, the partial sill as 0.00785807, and the total sill as 0.01396389. This method shows a moderate spatial dependence rate of 56.3%, with a range value of 5762 m, indicating a medium-sized effect distance. For the UK method, the nugget value was determined as 0.0012816100, the partial sill as 0.00013297, and the total sill as 0.00141458, showing a spatial dependence rate of 90.6%. This indicates weak spatial dependence, with EC values being more homogeneously distributed and a shorter effect distance of 3551 m. For the DK method, the nugget value was calculated as 0.0149452000, the partial sill as 0.03995901, and the total sill as 0.05490421, indicating a model with higher variation in EC values. The spatial dependence rate of 72.8% suggests moderate spatial dependence, with the range value of 9638 m reflecting a very large effect distance.

Overall, the findings suggest that soil pH values in the study area generally exhibit weak spatial dependence, whereas EC values show moderate spatial dependence. These results align with those of Zhao et al. (2024), who conducted a similar study on a European scale. In their research, they found that pH shows weak dependence on environmental variables but a stronger dependence on EC, which is attributed to differing soil processes. Moreover, they demonstrated that the spatial variation of pH is often associated with topography and carbonate content, while EC is more strongly influenced by salinity and climatic factors.

Table 2. Semivariogram parameters and spatial dependence ratios for different kriging methods for soil pH and EC values

	Model	Nugget	Partial Sill	Sill	Range (m)	Spatial Dependence (%)
pH	**Ordinary Kriging**	0.0000258017	0.00010771	0.00013351	5530	80.7%
	Universal Kriging	0.0011356647	0.00682873	0.0079644	5530	85.7%
	Disjunctive Kriging	0.2352803000	0.767537	1.0028173	5050	76.5%
EC	**Ordinary Kriging**	0.0061058190	0.00785807	0.01396389	5762	56.3%
	Universal Kriging	0.0012816100	0.00013297	0.00141458	3551	90.6%
	Disjunctive Kriging	0.0149452000	0.03995901	0.05490421	9638	72.8%

The optimal hyperparameters for the Level 1 Multi-Layer Perceptron (MLP) models are presented in Table 3. For both pH and EC values, various hyperparameter settings were tuned using GridSearchCV. In this study, to develop the final spatial models for soil pH and electrical conductivity (EC) characteristics, the input data consisted of the OK, UK, and DK values. For the Level 1 MLPpH model, the best performance was achieved with the following hyperparameters: 'relu' activation function, an α (L2 regularization term) of 0.001, a single hidden layer with 50 neurons, and the 'adam' solver. For the Level 1 MLPEC model, the lowest Mean Squared Error (MSE) was obtained with the 'tanh' activation function, an α of 0.0001, a single hidden layer with 100 neurons, and the 'adam' solver. These hyperparameter

selections ensured that the models generalized well according to the data characteristics and facilitated an efficient training process.

Table 3. Optimal Hyperparameters for Level 1 MLP Model

Model	Optimal Hyperparameters
Level 1 MLP_{pH}	{'activation': 'relu', 'alpha': 0.001, 'hidden_layer_sizes': (50,), 'solver': 'adam'}
Level 1 MLP_{EC}	{'activation': 'tanh', 'alpha': 0.0001, 'hidden_layer_sizes': (100,), 'solver': 'adam'}

3.3. Digital soil maps

The predicted spatial distribution maps for soil pH from the Level 0 base models (OK, UK, and DK) and the Level 1 meta-model (MLPpH) are shown in Figure 2. The numerical soil map for the MLPpH model displays the broadest spatial variation, capturing small-scale spatial changes, with a minimum value of 7.62, a maximum value of 7.92, and a standard deviation of 0.05. In comparison, the Level 0 models are ranked based on their ability to capture general trends and large-scale variations in pH values, with the following standard deviation values: UK (0.04), OK (0.03), and DK (0.01).

Soil pH maps for the study area, generated using different interpolation methods and modeling approaches, are presented in Figure 2. The OK method (a) reveals distinct spatial patterns in pH distribution, with smooth transitions. pH values range from 7.705 to 7.870, showing high pH values concentrated in the northern regions and lower pH values predominantly in the central and southern regions. The DK method (b) shows more pronounced spatial variability compared to OK, although its prediction range is narrower, from 7.693 to 7.833. This narrower range indicates reduced sensitivity to potential over-smoothing or outlier effects. The spatial locations of high and low pH regions are similar to those in the OK method, but the transition zones are less abrupt. The UK method (c) most effectively highlights the variability in pH values, with a broader pH range from 7.528 to 7.914. This method captures spatial gradients more clearly, with high pH areas concentrated in the northeast and low pH areas more prominent in the southwest.

The Level 1 MLPpH Model (d) provides smoother transitions in spatial patterns compared to other methods, with a prediction range from 7.619 to 7.926. This model effectively captures small-scale differences and potential extreme pH values in both the northern and southern regions in great detail. While the spatial patterns generally align with those of the other methods, the MLP model stands out for its ability to capture complex interactions in spatial relationships with greater flexibility.

Overall, all methods consistently identify high pH values in the northern/northeastern regions and low pH values in the southern/central regions. However, the sensitivity to transition zones and the approach to spatial dependency vary across methods. The UK method is particularly strong in detecting spatial gradients, making it a solid choice for capturing pH variations. The OK method offers a balanced and reliable approach for overall pH mapping, while the DK method may be preferred for reducing the impact of outliers. The MLP model excels in its flexibility to capture nonlinear spatial relationships. However, for the final selection of methods, it is recommended that validation using local data be performed to ensure accuracy.

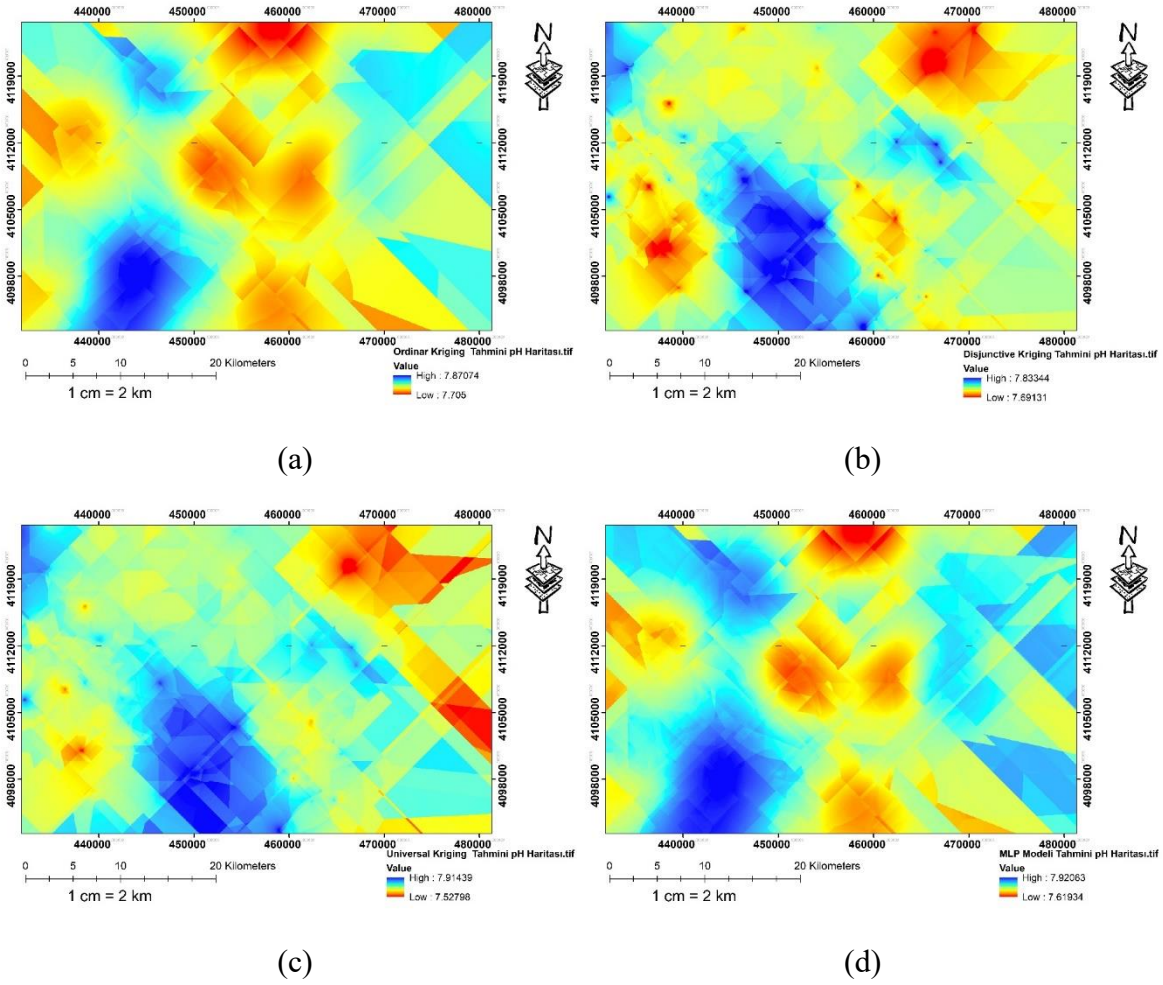

Figure 2. Digital soil maps for soil pH: a, b, and c correspond to Level 0 kriging interpolation methods—Ordinary Kriging, Disjunctive Kriging, and Universal Kriging, respectively. d represents the Level 1 MLP_{pH} model.

The predicted digital soil maps for soil EC are presented in Figure 3. The analysis of the soil EC maps highlights the spatial variability characteristics of the different methods used. The OK method predicted EC values ranging from 0.318 dS/m to 0.780 dS/m, providing smooth and balanced transitions. High EC values were concentrated in the southwest, while low EC values were predominantly observed in the northern and eastern regions. The DK method presented a similar distribution but showed more pronounced differences in transition zones. In this method, EC values ranged from 0.324 dS/m to 0.769 dS/m, with high EC areas more concentrated in smaller zones, while low EC areas expanded.

The UK method predicted EC values within a wider range, from 0.317 dS/m to 0.843 dS/m, reflecting spatial variability more distinctly. High EC concentrations in the southwest were defined in detail, and low EC areas were more prominent in the northeast. The Level 1 MLPEC model predicted EC values between 0.249 dS/m and 0.911 dS/m, offering a wider variation compared to other methods. Although the spatial patterns were generally consistent with OK and DK, the MLP model provided smoother transitions and better-defined high EC areas.

Overall, high EC values in the southwest and low EC values in the northern and eastern regions were consistently observed across all methods. OK and DK methods provided balanced and general predictions, while UK and the MLPEC model were more effective in capturing detailed spatial variations. UK stood out in defining

gradients and transition zones, while the MLPEC model flexibly captured nonlinear relationships and complex spatial patterns. The final choice of method should depend on the validation data and research objectives.

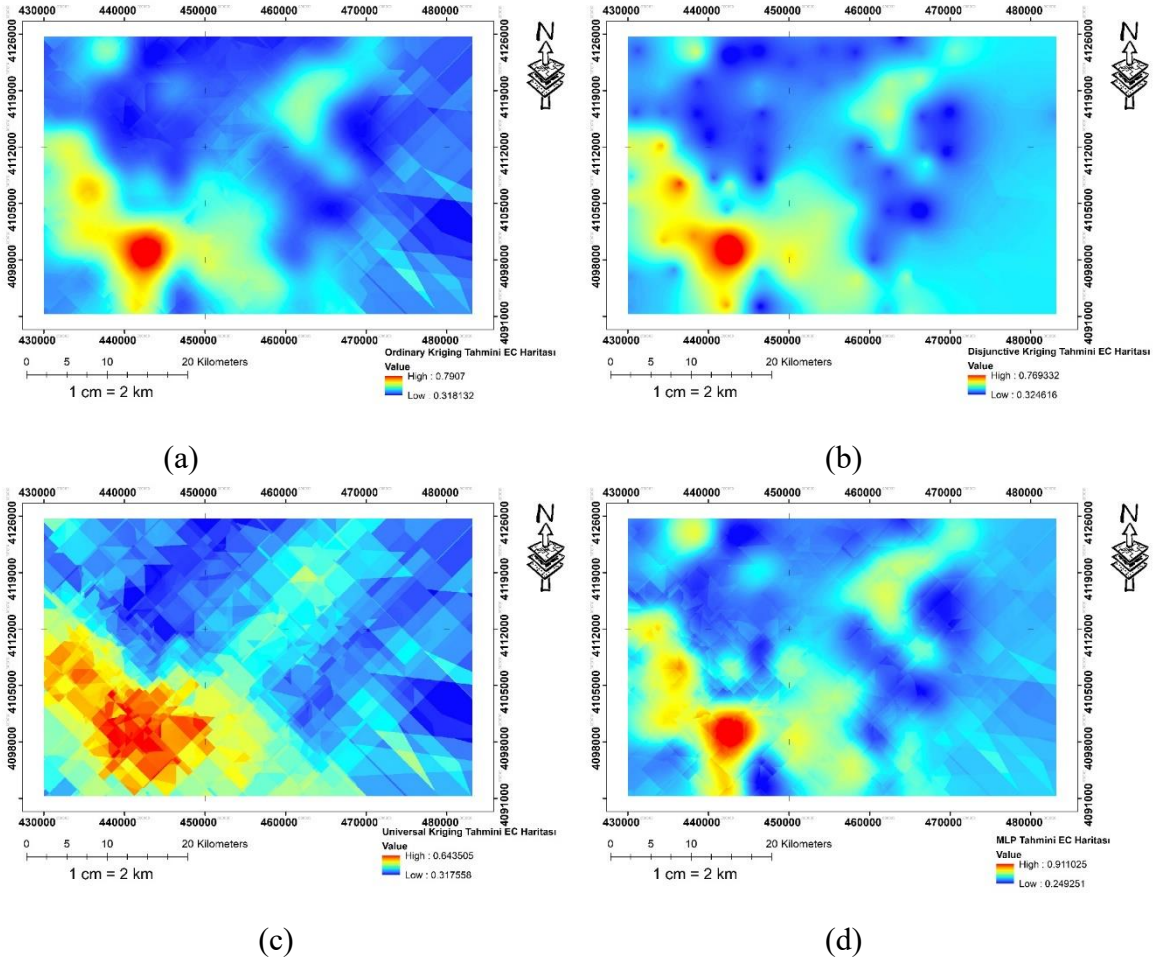

Figure 3. The digital soil maps for soil EC are presented as follows: Figure 3a shows the Level 0 Ordinary Kriging (OK) method, Figure 3b displays the Level 0 Disjunctive Kriging (DK) method, Figure 3c illustrates the Level 0 Universal Kriging (UK) method, and Figure 3d depicts the Level 1 MLPEC model.

The performance metrics of the four different models used for predicting the soil pH and EC values in the study area are provided in Table 4. For soil pH spatial prediction, the Level 1 MLP_{EC} model demonstrated the best performance with significantly lower MSE (0.001), MAE (0.0204), and RMSE (0.028), and the highest R^2 (0.858) values. The low MAE and RMSE values indicate that the model effectively minimized both systematic and random errors. The OK and DK methods showed reasonable accuracy in the training dataset, but the OK method performed poorly in pH predictions, as evidenced by its low R^2 value (0.103) and higher RMSE (0.081) and MAE (0.059) values. Furthermore, the OK method had the highest MSE (0.007), indicating low accuracy in pH predictions.

The UK method showed moderate accuracy in the training dataset (R^2: 0.546) but failed in the test dataset with a negative R^2 value (-0.880). The Level 1 MLPEC model, however, provided the best results in pH prediction with MSE (0.002), RMSE (0.040), and R^2 (0.715) in the test dataset. Meanwhile, the OK method performed

acceptably in the test dataset with R^2 (0.632), while the DK method showed lower accuracy (R^2: -0.309). The low R^2 in the training set and high R^2 in the test set of the OK method indicate that the model was prone to overfitting. Lu et al. (2023) performed soil pH mapping in Europe by combining multiple environmental variables with various machine learning algorithms. The study evaluated nine models (three linear and six nonlinear) for spatial prediction, using statistical metrics such as R^2, RMSE, and performance/deviation ratio (RPD) for model comparison. The results indicated that nonlinear machine learning models performed better than linear models in predicting soil pH. The random forest model achieved the best prediction performance with an R^2 value of 0.70, RMSE of 0.75, and RPD of 1.84.

In soil EC predictions, the Level 1 MLP_{EC} model outperformed all other methods, showing superior performance on both training and test data. The MLP_{EC} model achieved the highest accuracy on the training data with MSE (0.001), RMSE (0.031), and R^2 (0.900), and similarly provided the best results on the test data with MSE (0.002), RMSE (0.039), and R^2 (0.900). The OK method achieved high accuracy with R^2 (0.791) on the training data and R^2 (0.794) on the test data. However, it had relatively high RMSE (training: 0.0533; test: 0.0625) and MAE (0.0407) values, limiting error reduction. DK method showed moderate accuracy with R^2 values of 0.606 (training) and 0.624 (test), along with noticeable improvements in RMSE (0.0732) and MAE (0.0567). On the other hand, UK method showed the lowest performance in EC predictions, particularly on the test data, where it lagged behind other methods with MSE (0.012), RMSE (0.108), and R^2 (0.380).

Overall, the MLP model provided the best results across all metrics in both pH and EC predictions, demonstrating a clear advantage over the other methods. These results highlight the potential of modern methods in minimizing error rates for soil pH predictions. Shi et al. (2009) showed that the HASM method performed excellently in spatially predicting soil pH, particularly with low MAE (0.16) and RMSE (0.22) values. Similarly, the stacked machine learning model used in our study achieved significant success with low MAE (0.0204) and RMSE (0.028) values in pH predictions. Unlike HASM and other geostatistical methods, the meta-model approach was more flexible in modeling nonlinear relationships, further reducing error rates, and offering a method that could contribute to sustainable agricultural practices. The MLP model stands out with low MSE, RMSE, and MAE values, and its high R^2 values prove the explanatory power of the model. The R^2 metric used to evaluate pH and EC predictions in our study shows the proportion of total variance that the model can explain. Zhao et al. (2024) reported R^2 values of 0.70 for pH predictions and 0.53 for $CaCO_3$ predictions using the Extremely Randomized Trees (ERT) algorithm in their European-scale study. These values indicate that nonlinear models perform better than linear models in capturing complex environmental factors. The performance of the models in our study aligns with these findings. RMSE, used to evaluate model accuracy, provides the square root of the average of the squared differences between predicted and measured values. Zhao et al. (2024) reported an RMSE of 0.75 for pH predictions, demonstrating that the ERT algorithm achieved lower error rates, especially for pH predictions. The RMSE results used in our study indicate that the model performance is acceptable when compared with these reference values.

Among Kriging methods, DK generally performs better than OK and UK. In EC predictions, the OK method shows reasonable performance, but the MLP method stands out as the more powerful approach. Although DK provides reasonable results in some cases, its accuracy is not as high as that of the MLP

model. However, particularly in pH predictions, UK's weak performance on the test set limits the generalizability of the method. These findings highlight that the MLP model is the most suitable method for pH and EC predictions in terms of accuracy and reliability. The results suggest that deep learning-based approaches, such as MLP, outperform traditional spatial prediction methods, especially for complex and nonlinear data structures. Our study found that machine learning models demonstrated higher performance compared to geostatistical methods, with stacked models reducing error rates. This finding aligns with Zhao et al. (2024), whose European-scale study showed that nonlinear algorithms such as Random Forest performed better than classical methods like Kriging for pH and $CaCO_3$ predictions. Zhao et al. (2024) emphasized that nonlinear algorithms are more effective in capturing complex interactions of environmental variables, enhancing model performance.

In another study, Kshatriya et al. (2024) compared deep learning–multi layer perceptron (DL-MLP) and one-dimensional convolutional neural networks (1D-CNN) models and reported that the DL-MLP model performed better in pH predictions (R^2=0.30, RMSE=0.97). This finding is consistent with the accurate results of the Level 1 MLP models in our study. However, Kshatriya et al. (2024) noted that deep learning models are sensitive to high data requirements and that low sampling density could limit model accuracy. This observation corroborates the impact of data density on prediction accuracy observed in our study. Furthermore, the study supported the fact that DL-MLP models are particularly effective at capturing complex spatial patterns, which is reflected in the performance of pH and EC predictions in our study.

In a recent study, Kshatriya et al. (2024) analyzed model accuracies using metrics such as R^2 and RMSE for pH and organic carbon predictions and found that the DL-MLP model achieved reasonable accuracy in pH predictions (R^2=0.30, RMSE=0.97). When compared to the model accuracy values obtained in our study, these results reveal the potential of the DL-MLP model for predicting soil properties. The lower RMSE values from the models in our study suggest that machine learning algorithms can improve performance in regions where spatial variability shows more homogeneous distribution. However, the relatively low R^2 value in Kshatriya et al. (2024) study suggests that the effect of environmental variables on pH predictions might be limited, and including additional variables in the model could improve accuracy.

When evaluating the performance of soil pH and EC predictions, it is crucial to consider the MAE (Mean Absolute Error) values. MAE represents the average of the absolute differences between the predicted and actual values, providing a clear measure of the model's error magnitude. One of the key advantages of MAE is its lower sensitivity to the magnitude of errors compared to other metrics, as it treats all errors equally. This makes MAE particularly useful for realistic error assessment in models, as it is less influenced by outliers.

For pH predictions, the MLP model demonstrated the lowest MAE (0.020) on the training dataset, indicating the highest accuracy and reliability. The DK method achieved a similar MAE value of 0.020, though it lagged behind the MLP model in other performance metrics. The MAE for the UK method (0.029) was slightly higher, while the OK method had the highest MAE (0.059), indicating larger errors in predictions. On the test data, the MLP model again performed best with the lowest MAE (0.037), while the OK method showed a reasonable MAE (0.035). However, the UK method (0.074) and DK method (0.067) exhibited relatively high MAE values, indicating a significant increase in prediction error.

Table 4. Performance comparison of kriging methods and multi-layer perceptron (MLP) in pH and EC spatial prediction using

	Dataset	Method	MSE	RMSE	MAE	R^2
pH	Training	Ordinary Kriging	0.007	0.081	0.059	0.103
		Universal Kriging	0.003	0.058	0.029	0.546
		Disjunctive Kriging	0.002	0.047	0.02¹0	0.694
		MLP	0.001	0.028	0.020	0.858
EC		Ordinary Kriging	0.003	0.053	0.041	0.791
		Universal Kriging	0.009	0.095	0.074	0.331
		Disjunctive Kriging	0.005	0.073	0.057	0.606
		MLP	0.001	0.031	0.024	0.900
pH	Test	Ordinary Kriging	0.002	0.046	0.035	0.632
		Universal Kriging	0.011	0.104	0.074	-0.880
		Disjunctive Kriging	0.007	0.086	0.067	-0.309
		MLP	0.002	0.040	0.037	0.715
EC		Ordinary Kriging	0.004	0.062	0.047	0.794
		Universal Kriging	0.012	0.108	0.081	0.380
		Disjunctive Kriging	0.007	0.084	0.064	0.624
		MLP	0.002	0.039	0.028	0.900

For EC predictions, the MLP model again showed superiority in terms of MAE. On the training dataset, the MLP model achieved the best performance with the lowest MAE (0.024). The OK method (0.041) provided an acceptable MAE for EC predictions, while the DK method (0.057) and UK method (0.074) showed higher MAE values, indicating an increase in errors. On the test data, the MLP model continued to outperform the others with the lowest MAE (0.028), demonstrating greater consistency in its predictions. The OK method (0.047) also yielded a reasonable MAE on the test data, but the DK (0.064) and UK (0.081) methods exhibited higher MAE values, signaling increased prediction errors.

Overall, the MAE values confirm that the MLP model consistently provides the lowest error rates for both pH and EC predictions, establishing it as the most reliable method among the models tested. While the OK method produced reasonable results in terms of MAE, particularly on the test data, its performance was less impressive in other metrics. Conversely, the DK and UK methods showed weaker performance in terms of MAE, further highlighting the MLP model's superior accuracy. The robustness of MAE to outliers has allowed for a more realistic and reliable assessment of model performance, making it a crucial metric in evaluating the accuracy of the predictions. These findings underscore the MLP model's ability to consistently deliver reliable results with minimal error in both training and test datasets for pH and EC predictions.

Similarly, Vandana et al. (2024) investigated the spatial variability of soil pH and EC values in the South Telangana region of India, using a combination of kriging and machine learning techniques for digital soil mapping. The performance of the models was evaluated using RMSE, ME (Mean Error), and R^2 metrics. Their results showed that the Random Forest (RF) model outperformed traditional geostatistical methods, offering an effective tool for

spatial prediction of soil pH and EC. The RF model's high R^2 and low RMSE values indicated its reliability in digital soil mapping. A similar study by Tziachris et al. (2020) compared machine learning models (including Random Forest, Gradient Boosting, and Neural Networks) with geostatistical methods (Ordinary Kriging, Regression Kriging) for predicting soil pH. The study highlighted that low MAE could significantly enhance prediction accuracy, with the Gradient Boosting Kriging (GBKxgbT) model achieving an MAE of 0.177. In comparison, the MLP model in our study excelled in pH predictions, demonstrating low MAE (0.0204) and RMSE (0.028) values. These findings indicate that machine learning-based approaches, such as MLP, are highly effective in minimizing error rates and modeling nonlinear relationships, offering promising potential for improving soil property predictions.

Mousavi et al. (2023) identified significant performance differences between the integration of kriging and machine learning methods, which align with the findings in our study when evaluated using various error metrics. In their research, the RF-OK model, which models the kriging of random forest residues, demonstrated successful performance in pH predictions with an R^2 value of 0.82. Similarly, the MLP-ANN model in their study outperformed this approach, achieving a higher R^2 value of 0.858 and a lower RMSE value of 0.028 for pH predictions. This performance difference can be attributed to the MLP-ANN model's superior ability to capture nonlinear relationships and generalize more effectively, resulting in smaller error rates. In contrast, the RF-OK model excels in addressing large geographical variations and environmental variables, offering broader applicability, especially in diverse landscapes. The accuracy differences between these two models are influenced by factors such as dataset size, the impact of environmental variables on modeling, and the spatial dependence levels of the data.

Hybrid models, such as RF-OK and MLP-ANN, have shown significant improvements in prediction accuracy for pH and EC in the literature. Barikloo et al. (2024), in their study in the Urmia Plain, reported an R^2 of 0.82 and RMSE of 0.032 for the Random Forest (RF) model in pH predictions. However, by integrating kriging with the Random Forest model (RF-OK), they achieved an R^2 of 0.89 and reduced the RMSE to 0.007. Similarly, in our study, the MLP-ANN model outperformed traditional kriging methods, achieving an R^2 of 0.858 and an RMSE of 0.028 for pH predictions, showcasing the effectiveness of machine learning models in improving accuracy over conventional methods. These findings reinforce the potential of hybrid approaches in enhancing soil property predictions by leveraging the strengths of both machine learning and geostatistical techniques.

4. Conclusion

This study demonstrates that stacked machine learning models, particularly the Multilayer Perceptron (MLP) neural network meta-model, outperform traditional geostatistical methods in spatial predictions of soil pH and electrical conductivity (EC) values. The integration of the MLP meta-model with fundamental geostatistical methods, such as Ordinary Kriging (OK), Universal Kriging (UK), and Disjunctive Kriging (DK), has significantly enhanced prediction accuracy by reducing both systematic and random errors.

The MLP-based meta-model achieved an impressive R^2 value of 0.858 for pH predictions and 0.900 for EC predictions, demonstrating its superior performance compared to conventional geostatistical methods. The MLP model excelled at capturing small-scale spatial variations and nonlinear relationships, effectively minimizing key error metrics like RMSE and MAE. In contrast, methods like UK and DK displayed more limited generalizability in certain scenarios, which reduces their

suitability for sensitive decision-making processes, such as those in agriculture.

The findings from this study emphasize the potential of machine learning algorithms to significantly enhance the mapping of soil properties. These approaches not only improve prediction accuracy but also support the development of more reliable, detailed digital soil maps, which are essential for precision agriculture applications. By leveraging machine learning, agriculture can benefit from more precise insights into soil conditions, aiding in better-informed decision-making for sustainable farming practices.

5. Recommendations

To further enhance model accuracy, integrating environmental factors such as climate, topography, and vegetation into the predictive models is highly recommended. Incorporating such comprehensive datasets will not only improve the generalization ability of the predictions but also offer a deeper understanding of spatial variability in soil properties. Testing the proposed methods across different regions and soil types will provide valuable insights into their applicability in a broader geographic context, enabling a more thorough evaluation of the models' ability to adapt to regional dynamics.

For precision agriculture applications, the creation of high-resolution soil maps that highlight small-scale differences is essential. These maps will support more accurate and effective decision-making in land management, providing a practical tool for users in the agricultural sector. Additionally, training machine learning algorithms with more extensive and diversified datasets can further boost model accuracy. By utilizing larger datasets, models can better capture nonlinear relationships and improve prediction precision.

Finally, the development of user-friendly software and digital tools tailored for the agricultural sector is of great significance. These technologies will make the soil mapping process more accessible, empowering farmers and other stakeholders with the tools necessary for informed decision-making, ultimately supporting sustainable agricultural practices.

Declaration of Author Contributions

The authors declare that they have contributed equally to the article. All authors declare that they have seen/read and approved the final version of the article ready for publication.

Declaration of Conflicts of Interest

All authors declare that there is no conflict of interest related to this article.

References

Abakay, O., Günal, H. 2023. Ergani ovasında bazı toprak özelliklerinin mekânsal dağılımlarının belirlenmesinde lokal polinomal interpolasyon ve deneysel bayesyen kriging yöntemlerinin karşılaştırılması. *MAS Journal of Applied Sciences*, 8(4): 654-668.

Barikloo, A., Alamdari, P., Rezapour, S., Taghizadeh-Mehrjardi, R., 2024. Digital mapping of soil quality index to evaluate orchard fields using random forest models. Model. Earth Syst. Environ.

Butcher, K., Wick, A.F., DeSutter, T., Chatterjee, A., Harmon, J. 2016. Soil salinity: A threat to global food security. *Agronomy Journal*, 108(6): 2189-2200.

Cannone, N., Guglielmin, M., Malfasi, F., Hubberten, H.W., Wagner, D., 2021. Rapid soil and vegetation changes at regional scale in continental Antarctica. *Geoderma*, 394: 115017.

Durmaz, M., Günal, H., Budak, M., Çelik, İ., 2024. Harran Ovası'nda tarla ölçeğinde toprak fiziksel özelliklerinin mekânsal değişkenliği. *MAS Journal of Applied Sciences*, 9(2): 241-264.

Filippi, P., Cattle, S.R., Bishop, T.F., Odeh, I.O., Pringle, M.J., 2018. Digital soil monitoring of top-and sub-soil pH with bivariate linear mixed models. *Geoderma*, 322: 149-162.

Günal, H., Kılıç, M., Altındal, M., Gündoğan, R., 2021. Rapid spatial estimation of soil pH using machine learning under limited covariate conditions. *Levantine Journal of Applied Sciences,* 1(1): 30-37.

Haykin, S.S., 1999. Neural Networks: A Comprehensive Foundation, International edition. Prentice Hall.

Isaaks, E.H., Srivastava, R.M., 1988. Spatial continuity measures for probabilistic and deterministic geostatistics. *Mathematical Geology*, 20: 313–341.

Journel, A.G., Huijbregts, C.J., 1978. Mining Geo-statistics. London Acad. 600.

Kong, W., Chen, J., Zhu, P., 2024. Machine Learning-Based Uranium Prospectivity Mapping and Model Explainability Research. Minerals 14.

Kumar, V., 2007. Optimal contour mapping of groundwater levels using universal kriging—a case study. *Hydrological Sciences Journal*, 52: 1038–1050.

Ma, Z., Wang, P., Gao, Z., Wang, R., Khalighi, K., 2018. Ensemble of machine learning algorithms using the stacked generalization approach to estimate the warfarin dose. *PLoS One* 13.

Malvić, T., Balić, D., 2009. Linearity and Lagrange Linear Multiplicator in the Equations of Ordinary Kriging. *Naft Sciences Journal*, 60: 31–37.

Mesić Kiš, I., 2016. Comparison of Ordinary and Universal Kriging interpolation techniques on a depth variable (a case of linear spatial trend), case study of the Šandrovac Field. *The Mining-Geology-Petroleum Engineering Bulletin*, 31: 41–58.

Mousavi, A., Karimi, A., Maleki, S., Safari, T., Taghizadeh-Mehrjardi, R., 2023. Digital mapping of selected soil properties using machine learning and geostatistical techniques in Mashhad plain, northeastern Iran. *Environmental Earth Sciences*, 82: 234.

Oliver, M.A., Webster, R., Mcgrath, S.P., 1996. Disjunctive Kriging for Environmental Management. *Environmetrics*, 7: 333–358.

Pinkus, A., 1999. Approximation theory of the MLP model in neural networks. *Acta Numer,* 8: 143–195.

Somaratne, S., Seneviratne, G., Coomaraswamy, U., 2005. Prediction of soil organic carbon across different land-use patterns. *Soil Science Society of America Journal*, 69: 1580–1589.

Wackernagel, H., 2003. Multivariate Geostatistics: An Introduction with Applications, 3rd ed. ed, Heidelberg: Springer. Springer, Heidelberg.

Wang, R., 2018. Significantly Improving the Prediction of Molecular Atomization Energies by an Ensemble of Machine Learning Algorithms and Rescanning Input Space: A Stacked Generalization Approach. T*he Journal of Physical Chemistry A - ACS Publications*, 122: 8868–8873.

Webster, R., Oliver, M.A., 2007. Geostatistics for Environmental Scientists., 2 nd. ed, Vadose Zone Journal. NJ, United States.

To Cite: Öztürk, M., Kılıç, M., Günal, H., 2024. Digital Mapping of Soil pH and Electrical Conductivity: A Comparative Analysis of Kriging and Machine Learning Approaches. *MAS Journal of Applied Sciences,* 9(4): 1168–1185.
DOI: http://dx.doi.org/10.5281/zenodo.14542860.